CONF-8805141--1

DE88 011834

EVALUATION OF FRACTURE MODELS THROUGH PRESSURIZED-THERMAL-SHOCK TESTING

C. E. Pugh R. H. Bryan
B. R. Bass R. K. Nanstad
Oak Ridge National Laboratory
Oak Ridge, Tennessee 37831

DISCLAIMER

EVALUATION OF FRACTURE MODELS THROUGH PRESSURIZED-THERMAL-SHOCK TESTING*

C. E. Pugh R. H. Bryan
B. R. Bass R. K. Nanstad
Oak Ridge National Laboratory
Oak Ridge, Tennessee 37831

ABSTRACT

Two multiple-transient pressurized-thermal-shock experiments (PTSEs) have been conducted under the NRC-sponsored Heavy-Section Steel Technology (HSST) program. The first test (PTSE-1) employed an SA-508 class 2 steel with high Charpy upper-shelf energy level and a relatively high brittle-to-ductile transition temperature. The second test (PTSE-2) used a 2 1/4 Cr-1 Mo steel (SA-387 grade 22) that had been given a special heat treatment to yield a low Charpy upper-shelf energy level and attendant low tearing resistance. Each experiment included two combined thermal and pressure transients that gave rise to propagation and arrest of an initial long flaw that extended about 10% through the thick wall of the test cylinder. Both materials exhibited the ability to inhibit crack propagation by warm prestressing, high initiation toughness values and high crack-arrest toughness values. Cleavage initiation and arrest are modelled well by available fracture theories. However, calculations of ductile tearing based on resistance curves did not consistently predict the observed tearing.

1. INTRODUCTION

The pressurized-thermal shock experiments (PTSEs) in the Heavy-Section Steel Technology Program (HSST) are part of a carefully planned series of fracture mechanics experiments that are of a scale large enough to produce restraint at the crack tip similar to that of full-scale water-cooled nuclear reactor pressure vessels (RPVs). Hypothetical PTS transients, when imposed on the thick-wall vessel, produce high tensile stresses on the cooled inner surface. In addition, irradiation embrittlement is greatest near the inner surface, so that in the case of some pressurized-water-reactor vessels, pre-existing shallow flaws on the inner cooled surface may propagate in a fast fracture mode. If pressure is also present during the thermal transient, additional stresses are produced that become more dominant as the crack advances through the wall, and vessel integrity may be threatened in the absence of crack arrest or an action to reduce the load. The positive gradient in temperature and the lessening of neutron damage through the thickness provide increased material toughness to enhance crack arrest and terminate

*Research sponsored by the Office of Nuclear Regulatory Research, U.S. Nuclear Regulatory Commission under Interagency Agreements 0551-0551-A1 and 0552-0552-A1 with the U.S. Department of Energy under Contract DE-AC05-840R21400 with Martin Marietta Energy Systems, Inc.

an incident without breaching the vessel wall. The primary objective of the HSST PTSEs is to provide an experimental basis for the confirmation of current fracture analysis methods or for the development of new methods.

Fracture phenomena that can be investigated through these tests are:

1. ability of RPV steels to exhibit sufficiently high crack-arrest toughness to halt crack propagation before instability;
2. fracture mode transition as the crack propagates into ductile regions;
3. propensity for ductile tearing, prior to initial cleavage crack propagation;
4. inhibiting effects of warm prestressing on initiation of cleavage fracture; and
5. evolution of crack shape changes in clad vessels.

The first two experiments in this series (PTSE-1 and PTSE-2) were performed with flawed vessels of identical geometry (Fig. 1). In PTSE-1

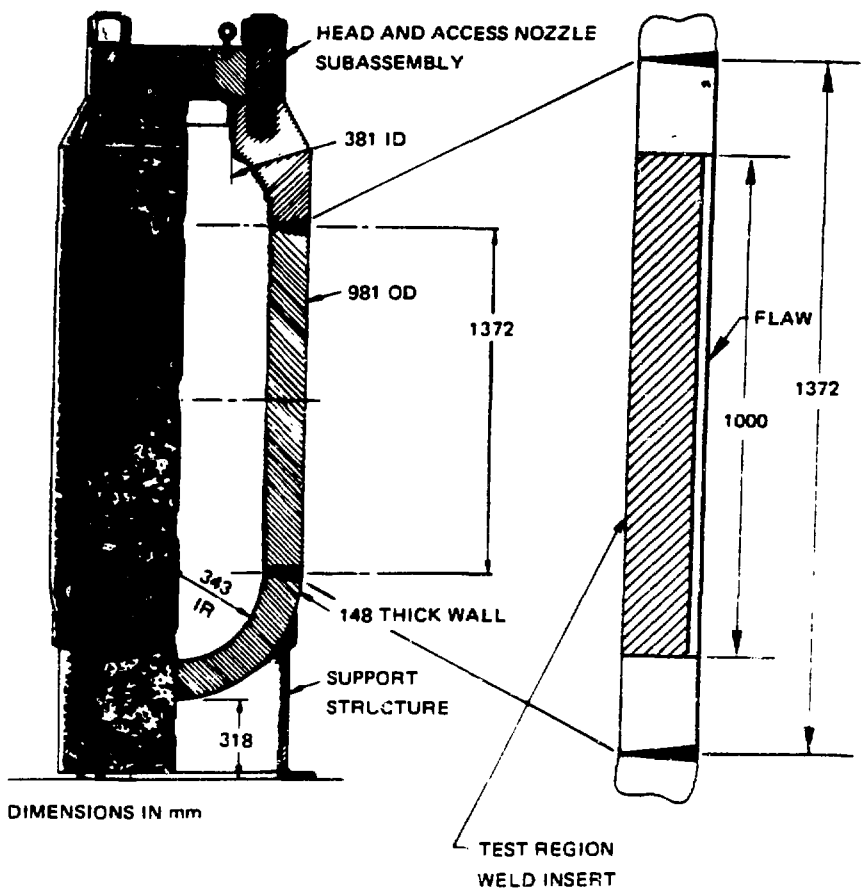

Fig. 1. PTSE test vessel geometry.

[1], the surface crack was embedded in a welded-in plug of specially tempered forged steel that, with normal heat treatment, would have met the specifications for SA-508 class 2 steel. The objectives of PTSE-1 were to investigate the effects of warm prestressing and the nature of arrest of a rapidly propagating crack at temperatures that are near or above the temperature corresponding to the onset of the Charpy (ductile) upper shelf [1]. PTSE-1 clearly demonstrated that crack propagation was strongly inhibited during phases of warm prestressing in which the stress intensity factor K_I was decreasing with time ($\dot{K}_I < 0$) or when K_I was much lower than an earlier maximum. PTSE-1 also demonstrated that the test material exhibits very high crack arrest toughness at high temperatures, exceeding the implied limit of 220 MPa $\sqrt{m}$ of Sect. XI of the *ASME Boiler and Pressure Vessel Code* [2], and that arrest could occur in a positive K_I gradient.

The second experiment [3] (PTSE-2) was concerned, primarily, with characterizing crack propagation in material with low Charpy upper-shelf energy level and, secondarily, with warm prestressing. The test material in PTSE-2 was a specially heat treated 2 1/4 Cr-1 Mo plate, meeting SA-387 grade 22 specifications with a low Charpy impact energy (~50 to 70 J) on the ductile upper shelf, which ensured low ductile-tearing resistance. Vulnerability of existing reactor pressure vessels to damage in overcooling accidents is a potential problem mainly in instances of vessel steels that have high copper contents and, consequently, high susceptibility to fast-neutron embrittlement. Coincidentally, these high-copper steels have low ductile tearing resistance at temperatures on the Charpy upper shelf [4]. While conclusions from overcooling accident analyses are principally determined by transition temperature and its effect on crack initiation, in some hypothetical transients crack arrest is the controlling phenomenon. Crack-arrest toughness in low-upper-shelf steels has been presumed to have the same dependence on temperature (T) and the reference temperature for the nil ductility transition (RT_{NDT}) as do steels with high upper-shelf toughness, but this has not been established experimentally. Furthermore, structural validation is needed of the post-arrest behavior of an arrested crack relative to ductile tearing, particularly if the tearing resistance, J_R, is low.

The PTSE-2 experiment was designed to examine crack propagation and arrest in a material that exhibits low tearing resistance. One phase of the experiment was defined to produce cleavage arrest at temperatures above the onset of Charpy upper-shelf behavior followed by unstable tearing. Another objective was to achieve cleavage initiation of a warm-prestressed crack, a goal which was not accomplished in PTSE-1. A third consideration was to evaluate tearing resistance models through interpretation of stable tearing that occurs prior to cleavage initiation and after arrest.

This paper presents a brief description of the pressurized-thermal-shock test facility at ORNL, a review of the test objectives and a summary of the test results. Results from analyses of PTSE-1 and -2 are compared

with the experimental observations. Consideration is given to the cleavage run-arrest events that occurred and to the various ductile tearing phases of each test. Finally, some conclusions are presented based on the outcome of the studies.

2. GENERAL DESCRIPTION OF TESTS

The details of the test vessel and flaw geometry are shown in Fig. 1 and in Table 1 for both PTSE-1 AND -2 tests. An HSST intermediate test vessel was used as a tough carrier vessel and prepared with a plug of specially heat treated test steel welded into the vessel. The 1-m-long sharp flaw was implanted in the outside surface of the plug by cracking a shallow electron-beam weld under the influence of hydrogen charging. For each test, the vessel was extensively instrumented (e.g., see Fig. 2) to give direct measurements of crack-mouth opening displacement, temperature profiles through the vessel wall, and internal pressure during the transient. The data were recorded to permit analysis of the temperatures that control the thermal stress states; the temperatures that define the fracture-toughness conditions along the tip of the crack; the internal pressure, which defines the stress states from mechanical loading; and the displacements along and near the crack, which can be used to estimate crack depth and length.

Table 1. Geometric parameters of PTSE vessels

Parameter	PTSE-1 value	PTSE-2 value
Inside radius, mm	343	343
Wall thickness (w), mm	147.6	147.6
Flaw length, mm	1000	1000
Flaw depth (a), mm	12.2	14.5
a/w	0.083	0.098

In each experiment, the flawed vessel was enclosed in an outer vessel as shown schematically in Fig. 3. The outer vessel is electrically heated to bring the test vessel to the desired uniform initial temperature of about 290°C. A thermal transient is initiated by suddenly injecting chilled water or a methanol-water mixture through an annulus between the test vessel and the outer vessel. The annulus between the vessel surfaces was designed to permit coolant velocities that would produce the appropriate convective heat transfer from the test vessel for a period of about 10 min. Pressurization of the test vessel is controlled independently by a system capable of pressures up to about 100 MPa. A detailed description of the ORNL PTS test facility, including the main coolant and pressurization systems, as well as the computer-controlled data acquisition systems, is given in Refs. 1 and 3.

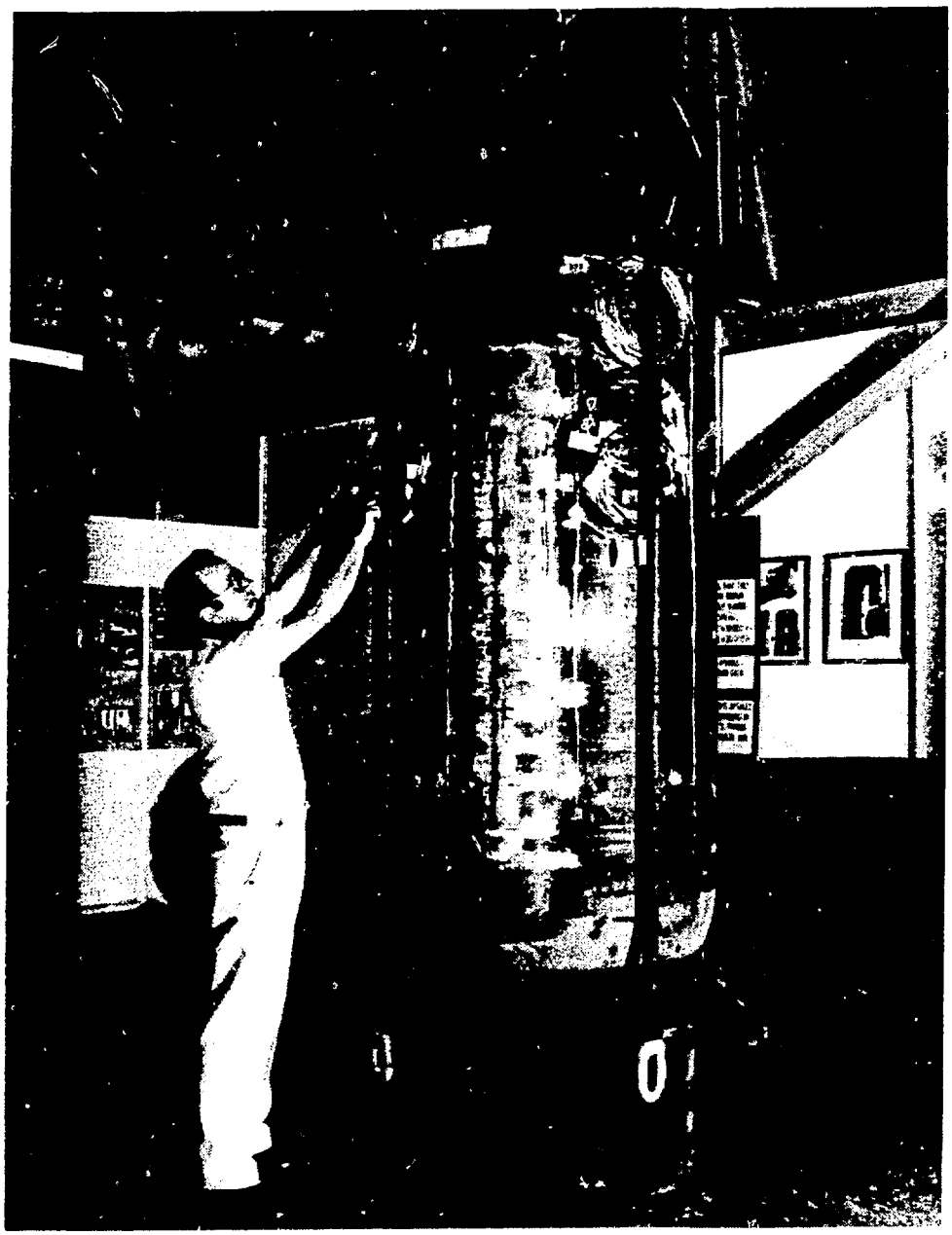

Fig. 2. PTSE vessel showing crack-mouth-opening displacement gage installation.

Extensive material properties tests and fracture analyses preceded the transient test of each of the PTSE vessels. The tests were performed in three (PTSE-1) phases or two (PTSE-2); in each phase the vessel was initially in an isothermal state (~290°C). Each phase consisted of a pressure transient and a thermal transient, which were coordinated to produce an evolution of stress and toughness states that would fulfill the objectives of the plan. Fracture analyses performed to define the

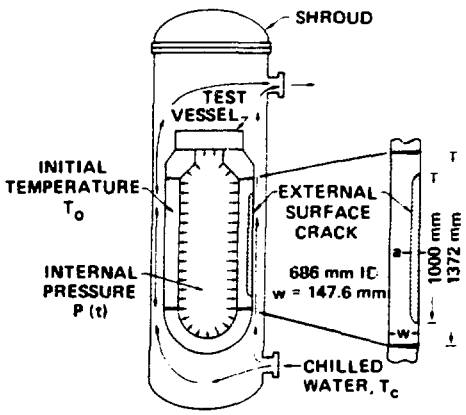

Fig. 3. Schematic view of pressurized-thermal-shock vessel inside shroud.

transients were based on fracture-toughness data from tests of small specimens. Much of the run-arrest portions of the expected crack jumps was expected to take place in a temperature range above that for which the small specimens could provide data; consequently, the transients were selected to attain the desired objectives in the presence of uncertainty. The ORMGEN/ADINA/ORVIRT system [5-7] of finite-element computer programs was used in conjunction with the OCA/USA program [8] to define fracture properties and transients that would meet the PTSE objectives.

The first phase of both the PTSE-1 and -2 tests involved coordinated pressure and temperature transients which made the initial crack supercritical ($K_I > K_{Ic}$) while in a warm prestressed state, as shown schematically in Fig. 4. As described in the following sections, the loading in the antiwarm prestressing phase of PTSE-1 was not sufficient to

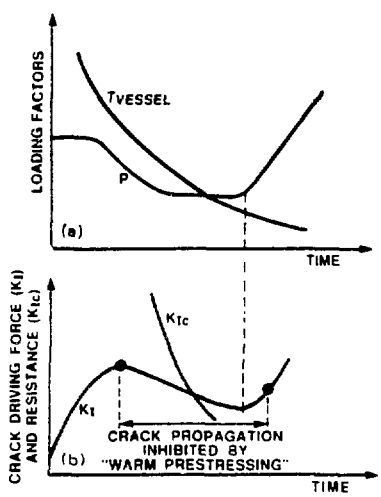

Fig. 4. Warm prestressing phase induced by PTSE transient loading: (a) loading factors of pressure and temperature; (b) crack driving force and fracture resistance during warm prestressing phase.

produce crack initiation; however, crack initiation was achieved in this phase of the PTSE-2 test.

3. EXPERIMENT PTSE-1 (SA-508 STEEL)

Properties of the PTSE-1 test material are given in Table 2 and in Figs. 5 and 6. Fracture initiation and arrest toughnesses were determined from tests of 25 mm and 37 mm compact specimens, respectively. Figures 5 and 6 show the K_c and K_a data together with size-effect-adjusted data [9] and the curves used in fracture analyses. The A curve in Fig. 5 was used in analyses made prior to execution of the first transient (PTSE-1A), and curve B was used subsequently. The initiation-toughness data in Fig. 5 were obtained by the Babcock and Wilcox Research Center and the arrest-toughness data in Fig. 6 by the Battelle Columbus Division in support of this program.

Table 2. Tensile and fracture properties for PTSE materials

Property	PTSE-1 value	PTSE-2 value
Yield strength, MPa	600	255
Ultimate strength, MPa	750	518
NDT temperature, °C	66	49
Onset of Charpy upper shelf (100% shear fracture appearance), °C	150	150
Charpy upper shelf Energy, J	~115	~50—75[a]
Charpy transition temperature, °C		
At 50% shear fracture appearance	~100	90
At 0.89-mm lateral expansion	~100	98

[a]Range for all depths in plate. The average at 1/4 depth is ~68 J.

The pressure and thermal transients for the three phases (A, B, and C) of the experiment are given in Fig. 7 and Table 3. For the A test, the K_I trajectory reconstructed from experimental data is shown in Fig. 8. Since temperature (on the abscissa) decreases monotonically with time, one can discern from this plot two episodes of simple warm prestressing ($\dot{K}_I < 0$), while K_I is greater than K_{Ic}. Because of the inhibiting influences of warm prestressing, the crack did not propagate during the A transient.

Plans for the B and C transients were based upon the evidence from test phase A that the vessel insert was tougher than originally estimated and

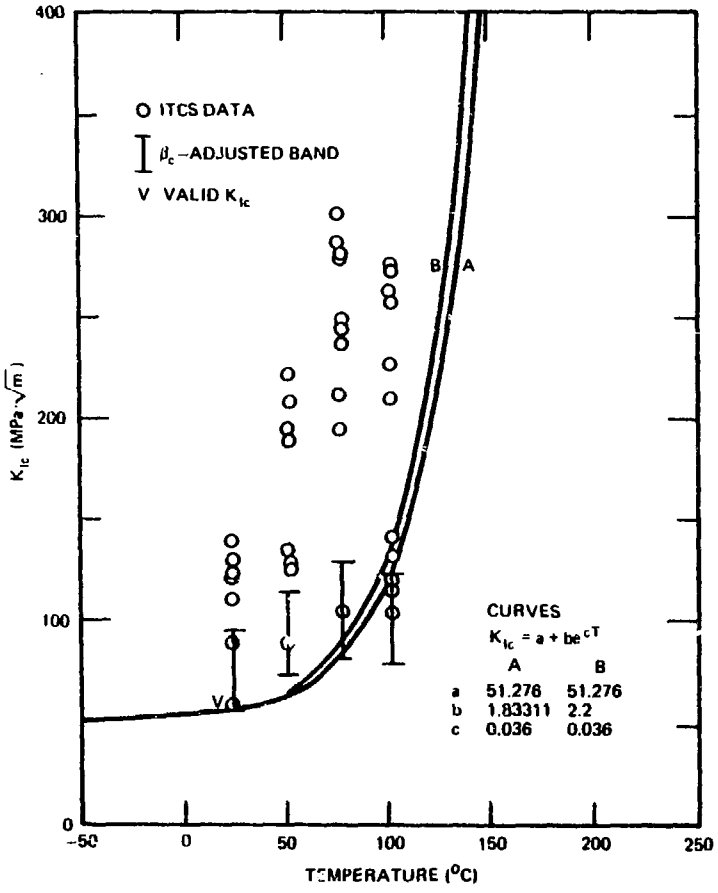

Fig. 5. Fracture initiation toughness values obtained from laboratory specimen tests. (Curve A used in pretest analyses for PTSE-1A and Curve B used subsequent to performing PTSE-1A.

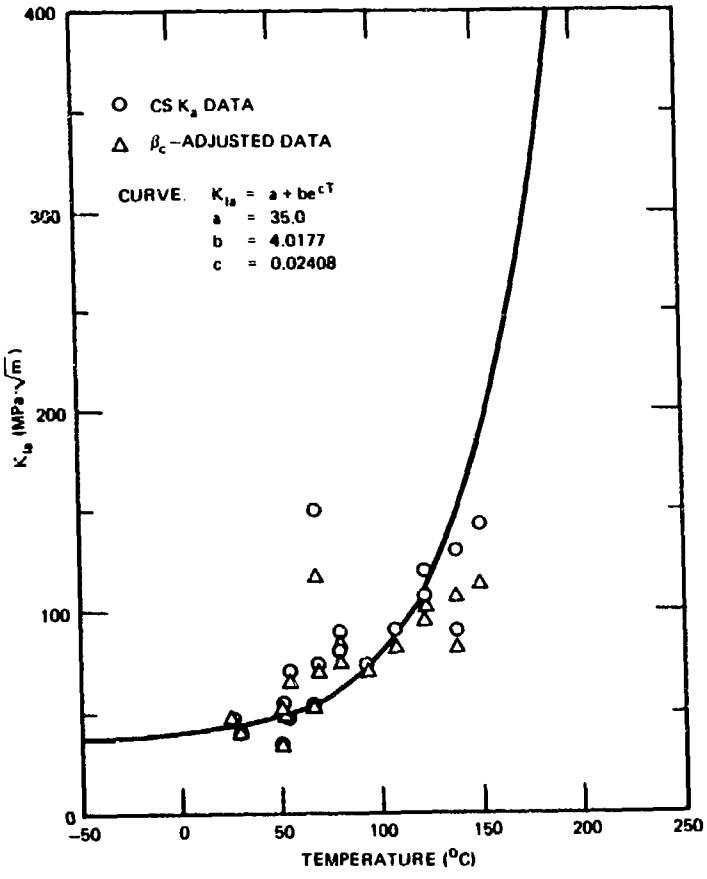

Fig. 6. Crack-arrest toughness values obtained from laboratory specimen tests. (CS) data are from 37-mm-thick compact specimens, and the curve is a least-squares fit to the size-effect-adjusted data with the highest point at 67°C excluded.

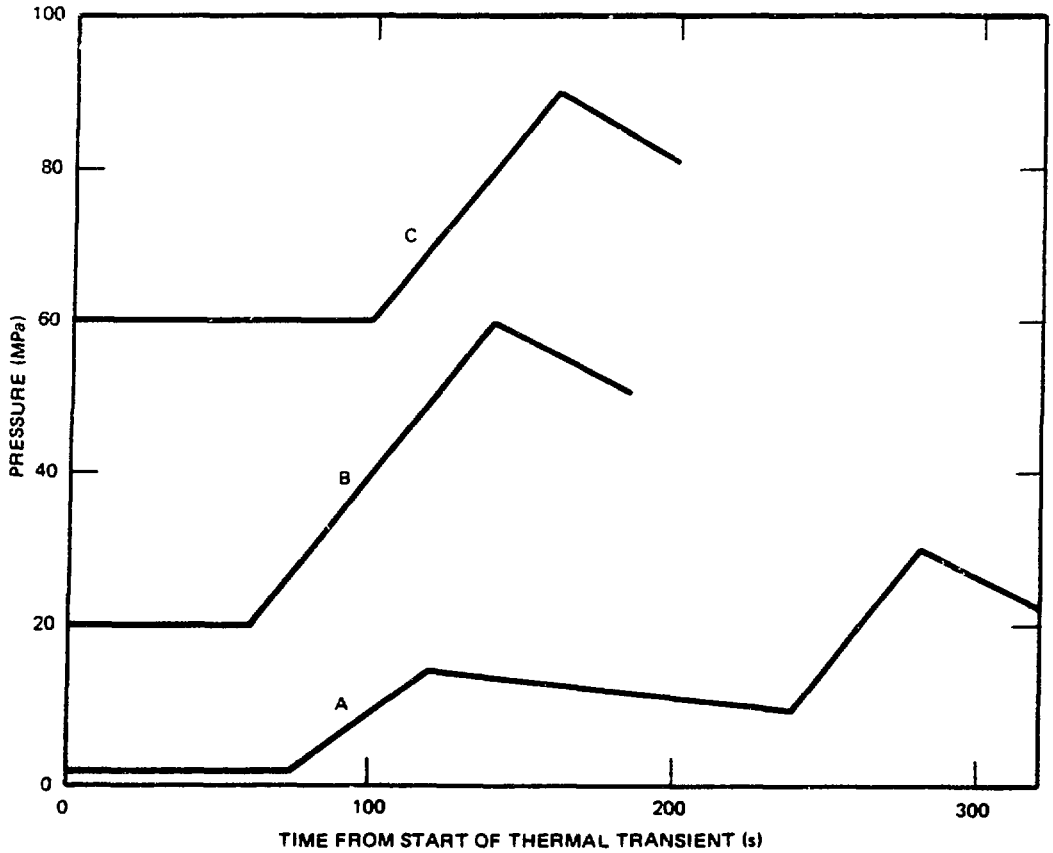

Fig. 7. Planned pressure transients for PTSE-1A, -1B, and -1C.

Table 3. Conditions for PTSE-1A, -1B, and -1C transients

	Test Transients		
	PTSE-1A	PTSE-1B	PTSE-1C
Thermal transient parameters			
Initial vessel temperature, °C	277.6	290.7	287.4
Coolant temperature T(t), °C	15-34[a]	-22-0[a]	-29-14[a]
h(t), $W \cdot m^{-2} \cdot K^{-1}$	8000-6000[a]	5500-6500[a]	4000-5500[a]
Pressure transient (planned)	Curve A, Fig. 7	Curve B, Fig. 7	Curve C, Fig. 7
Initial flaw depth			
a, mm	12.2	12.2	24.4
a/w	0.083	0.083	0.165

[a]Initial and final (t ≈ 300 s) values.

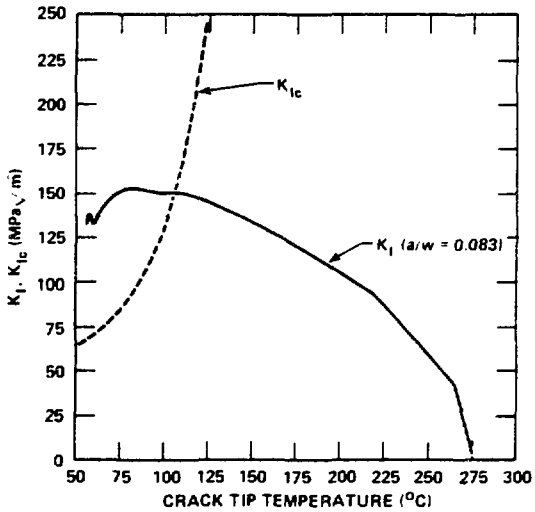

Fig. 8. Results of OCA/USA analysis of PTSE-1A based on measured temperature, pressure and flaw depth. The K_{Ic} expression is curve B of Fig. 5.

that, to overcome warm prestressing, a higher K_I value would have to be attained. Accordingly, the B curve of Fig. 5 was adopted for further analysis, lower coolant temperatures were specified for the thermal transient (Table 3), and a higher pressure transient was selected (curve B, Fig. 7). A two-step pressure transient was not performed during PTSE-1B test because a second pressure increase of a useful magnitude was not within the capabilities of the pressurization system. The B transient resulted in a crack jump to a depth of 24.4 mm. The conditions of initiation and arrest from an analysis performed with OCA/USA are shown in Fig. 9.

The final transient, PTSE-1C, was performed under the conditions given in Table 3 and with the planned pressure transient described by curve C in Fig. 7. The crack jumped to a depth of 41 mm under conditions presented in Fig. 10.

The vessel was examined visually and ultrasonically after the C transient. At the outside surface the crack extended axially about 110 mm at the upper end of the vessel and about 120 mm at the lower end. The crack branched at the lower end and the instrumentation indicated that all of the axial extensions occurred in transient PTSE-1B.

The flawed region was cut from the vessel, chilled in liquid nitrogen, and broken apart to reveal the fracture surfaces, one segment of which is shown in Fig. 11. Details of all the segments of the fracture surface are discussed in Ref. 1. Fractographic examination of the surfaces and measurement of the flaw geometry indicated that the initial flaw tore slightly prior to the initial cleavage fracture. The initial crack

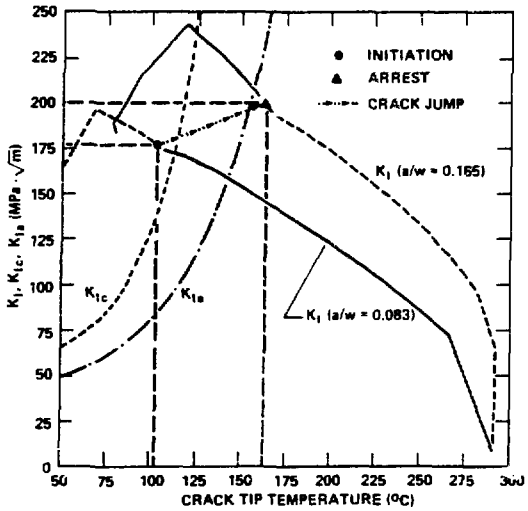

Fig. 9. Results of OCA/USA analysis of PTSE-1B based on measured temperature, pressure, flaw depth, and time of crack jump.

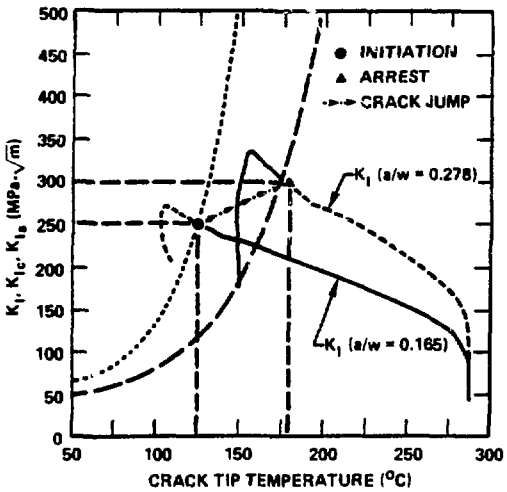

Fig. 10. Results of OCA/USA analysis of PTSE-1C based on measured temperature, pressure, flaw depth, and time of crack jump.

extension was essentially a pure cleavage fracture throughout the first half of the extension and predominantly cleavage (~90%) with finely dispersed ductile tearing in the remaining extension. The crack extension in the second crack jump was mixed mode throughout with about 85% cleavage. At the ends of the two crack extensions there were no coherent regions of ductile tearing, contrary to predictions based on the measured tearing resistance J_R of the material.

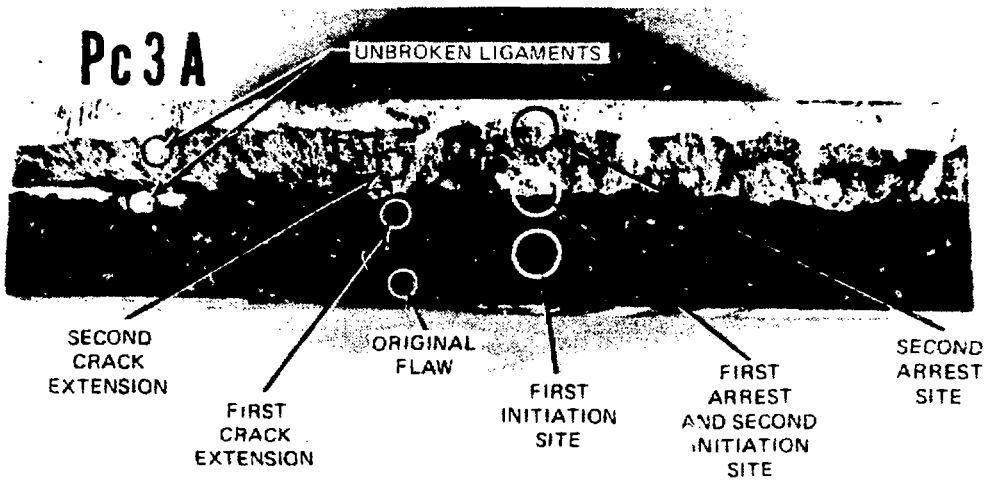

Fig. 11. Typical portion of fracture surface from PTSE-1.

Initiation and arrest toughness from quasi-static calculations are summarized in Table 4 for the three phases of the experiment (PTSE-1). The values of K_{Ic} and K_{Ia} inferred from test data are shown in Fig. 12 in comparison with the pretest estimates and with the K_{Ic} and K_{Ia} relationships suggested in Sect. XI of the ASME *Boiler and Pressure Vessel Code*. As can be seen from Fig. 12, the pretest estimates of fracture toughness are reasonably close to the PTSE-1 values.

Table 4. Summary of fracture conditions in PTSE-1

Experiment	Event	Crack depth (mm)	Crack depth ratio (a/w)	Crack tip temperature (°C)	K_I (MPa•$\sqrt{m}$)
PTSE-1A	1st max K_I (at $K_I \approx K_{Ic}$)	12.2	0.083	105	152
	2nd max K_I	12.2	0.083	78	154
	3rd max K_I	12.2	0.083	57	139
PTSE-1B	Initiation	12.2	0.083	104	177
	Arrest	24.4	0.165	163	201
	Subsequent max K_I	24.4	0.165	118	247
PTSE-1C	Initiation	24.4	0.165	125	254
	Arrest	41	0.278	179	299
	Subsequent max K_I	41	0.278	156	340

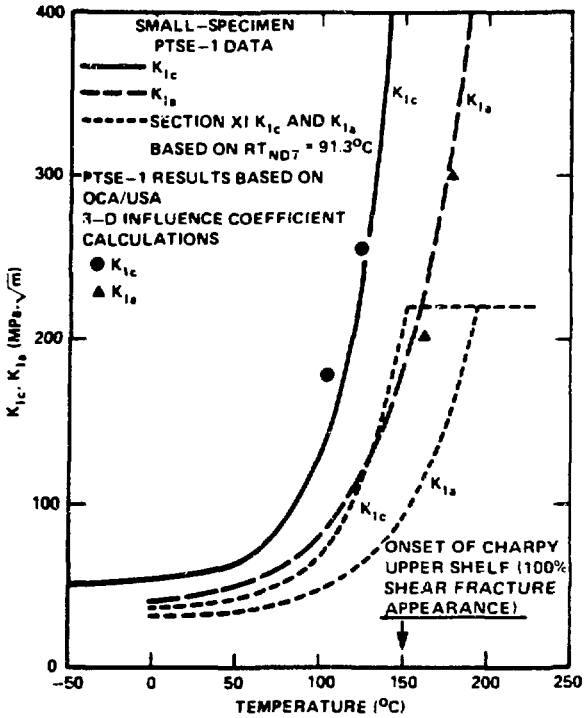

Fig. 12. Comparison of PTSE-1B and -1C results with curves representing small-specimen K_{Ic} and K_{Ia} data and ASME Section XI curves.

4. EXPERIMENT PTSE-2 (LOW CHARPY UPPER-SHELF ENERGY STEEL)

In PTSE-2, the insert (test) material was taken from a 2 1/4 Cr-1 Mo plate, meeting SA-387 grade 22 specifications. The two pieces used for the insert and for properties characterization were exposed to the same heat treatment after the insert was welded into the vessel. The heat treatment was intended to provide tensile and toughness characteristics favorable for the experimental requisites. The tensile strengths were undesirably low, but other properties, although somewhat uncertain, were satisfactory. The properties determined prior to the experiment are summarized in Table 2.

The tearing resistance of the characterization piece (PTC1) is presented in Fig. 13, which shows tearing resistance (J_R) vs incremental crack depth (Δa) for the specimens that exhibited the highest and lowest resistance. Figure 13 also compares these data with the highest and lowest tearing resistances measured for a class of irradiated high-copper welds [10,11]. With respect to tearing resistance, Fig. 13 shows that the PTSE-2 material was representative of the type of material that is of greatest concern in evaluation of overcooling accidents.

The design of the thermal and pressure transients for the PTSE-2 experiment required estimates of crack initiation and arrest toughnesses.

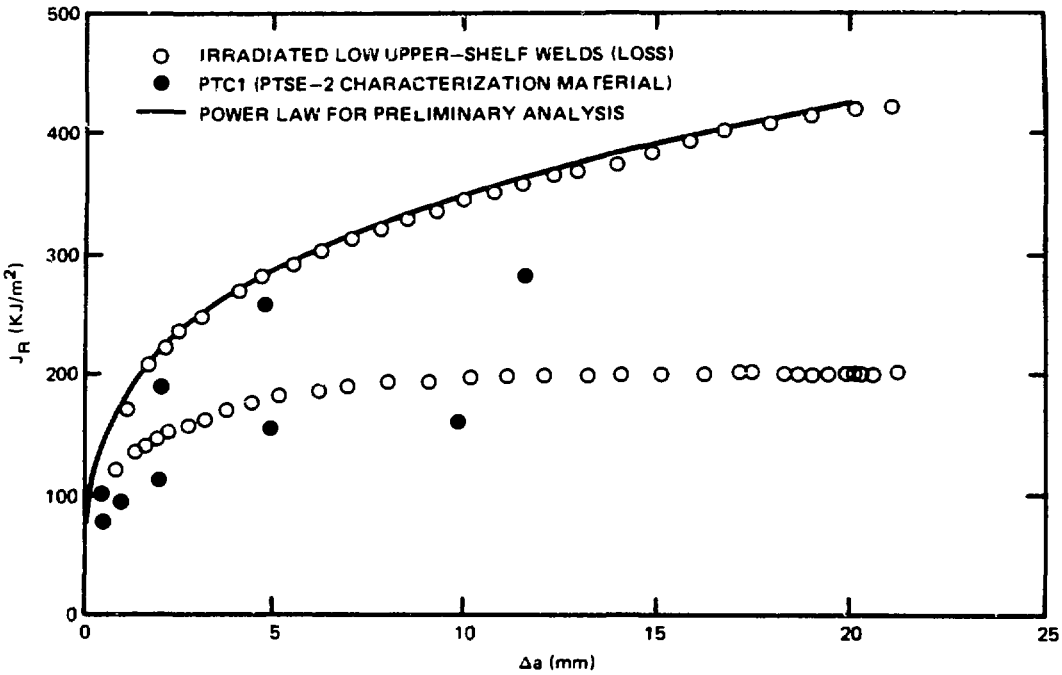

Fig. 13. Tearing resistance J_R vs crack extension Δa for PTC1, the characterization material for low-upper-shelf insert in PTSE-2 vessel. PTC1 data are compared with data from tests of irradiated high-copper welds. Plotted points are for highest and lowest J_R curves for each of two materials.

Pretest crack-arrest (K_{Ia}) and fracture-toughness (K_{Ic} and K_J) data are shown in Figs. 14 and 15, respectively. The K_{Ia} data were obtained from tests of 33- and 51-mm-thick specimens. K_{Ic} and K_J data are from tests of 25-mm-thick compact specimens. From PTSE-1 experience [1], it was expected that the K_{Ia} data would provide the most reliable indication of fracture toughness at high transitional temperatures. Therefore, the K_{Ia} data were evaluated first, and the upper- and lower-toughness curves shown in Fig. 14 were determined by least-squares fits to the raw K_{Ia} data and to β-adjusted [9] data, respectively. The curves representing K_{Ic} at high transitional temperatures were presumed, in the absence of reliable data, to be ~30°K from the respective K_{Ia} curves. It transpired that a curve determined by the low-temperature K_{Ic} points and fitting β and rate-adjusted K_J data [1,9] in the transition was suitably related to the upper K_{Ia} curve. This fitted K_{Ic} curve and a lower-toughness K_{Ic} curve, displaced by 30°K from the former (Fig. 15), were adopted for planning the PTSE-2 experiment.

The experiment was planned to consist of two transients, of which the first would induce warm prestressing ($\dot{K}_I < 0$) followed by reloading ($\dot{K}_I > 0$) until the crack propagated by cleavage. The second transient was planned to produce a deep cleavage crack jump with an arrest or mode conversion occurring only after conditions conducive to unstable tearing

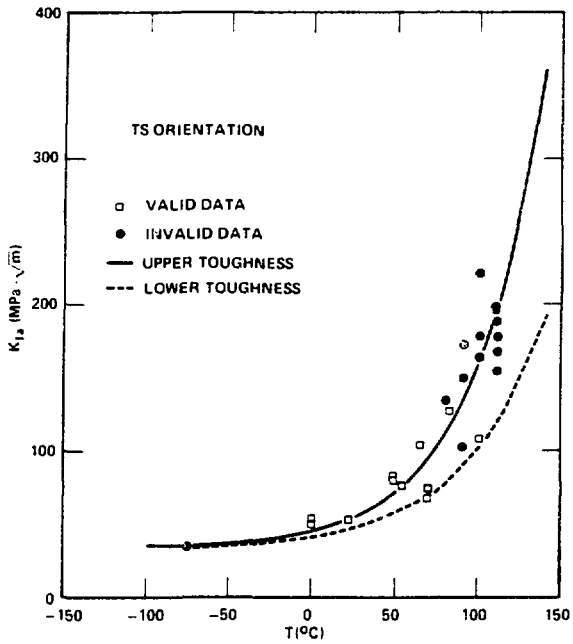

Fig. 14. Crack-arrest toughness data for characterization piece PTC1. Upper-toughness curve is least-squares fit to data shown. Lower-toughness curve is similar fit to β-adjusted data (points not shown).

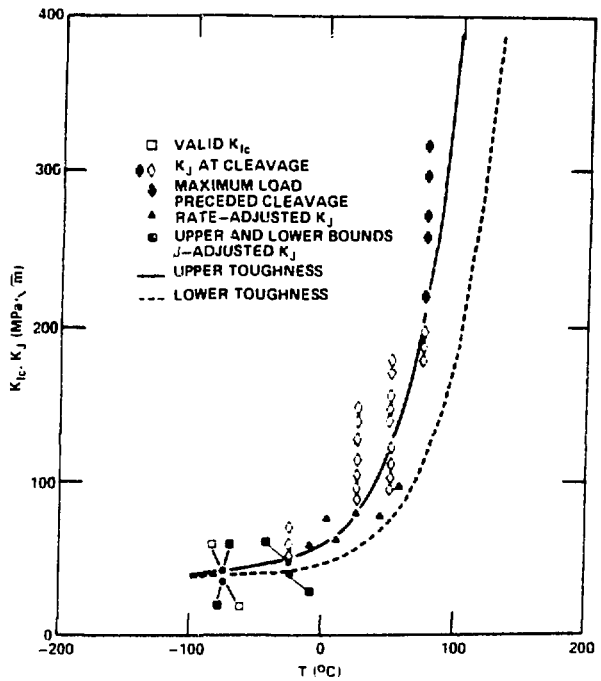

Fig. 15. Fracture toughness data for characterization piece PTC1. Two lowest points are only valid K_{Ic} data. Upper-toughness curve is least-squares fit to β-adjusted and rate-adjusted points.

were attained. The second transient was also necessary to provide a measurement of K_{Ic} that was not strongly affected by warm prestressing so that the effects of warm prestressing in the first transient could be evaluated.

The concurrent pressure and temperature transients along with the crack-mouth-opening displacements vs time data are fully discussed in Ref. 3. The fracture behavior throughout the experiment was resolved into events that were evident in the CMOD recordings and in the distinct stages of fracture visible on the fracture surfaces. Ductile tearing occurred in three separate phases of PTSE-2A: (1) prior to warm prestressing ($t < 184.6$ s); (2) during reloading (341.8 s $< t <$ 361.4 s); and (3) after the cleavage arrest ($t > 361.4$ s). The crack propagated both axially and radially by cleavage at 361.4 s. In the second transient PTSE-2B, K_I increased monotonically, while the crack tore stably, propagated radially in cleavage, and tore unstably. The phases of fracture in both transients are shown by the photograph of the fracture surface in Fig. 16. The final tearing ruptured the vessel over an axial distance of ~730 mm. The important events and conditions of PTSE-2 are summarized in Table 5 along with calculated K_I values.

Fracture analyses were performed by methods of linear-elastic fracture mechanics and by two- and three-dimensional elastic-plastic finite-element analysis. Pretest analysis was based on calculated temperature distributions and prospective pressure transients attainable with the test facility. Post-test analysis was based on measured pressures and temperatures. Results reported here are all based on a two-dimensional elastic-plastic finite-element analysis performed by using the ADINA/ ORVIRT system of computer programs.

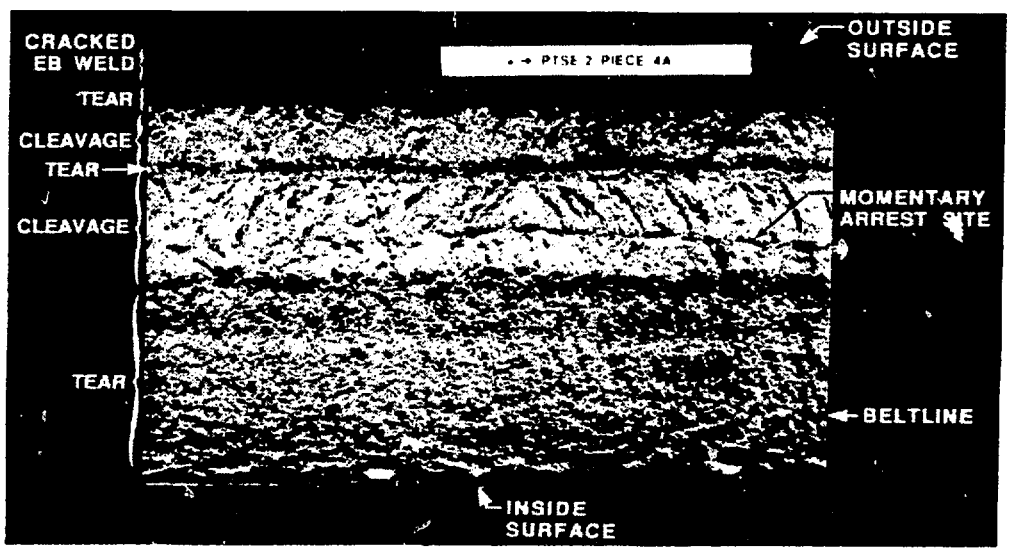

Fig. 16. Photograph of central segment of PTSE-2 fracture surfaces.

Table 5. Events and conditions during the PTSE-2 transients

Event	Time (s)	Crack depth (mm)	Crack-tip temperature (°C)	K_I (MPa•$\sqrt{m}$)
	PTSE-2A			
Initiation of thermal shock	~112	14.5	302.8	
First maximum K_I	184.6	19.6	128.0	195.7
Minimum K_I	341.8	19.6	77.0	171.0
Onset of secondary precleavage tearing	341.8	19.6	77.0	171.0
Initiation of cleavage	361.4	22.5	80.7	198.9
Cleavage arrest	361.4	39.3	130.6	261.4
Termination of tearing (by unloading)	365.6	42.4	138.0	278.7
	PTSE-2B			
Initiation of thermal shock	~155	42.4	274.9	
Onset of precleavage tearing	<575.8	42.4	*a*	*a*
Initiation of cleavage	575.82	46.1	102.4	248.1
Interruption of cleavage by ductile tearing and reinitiation		60.2	146.8	361.6
Final cleavage arrest	575.82	78.8	162.9	419.3
Onset of ductile tearing	576.2	78.8	162.9	406.5
Vessel rupture (and complete unloading)	576.7	147.6	216.4	

[a] At t = 575.82 s, T = 94.8°C, and K_I = 233.8 MPa•$\sqrt{m}$ at this depth.

The course of transient PTSE-2A is shown in Fig. 17 in terms of a plot of K_I and K_{Ic} vs time. Prior to initial warm prestressing (the period from point A to B), the crack tore from its initial depth (a_1 = 14.5 mm) to the intermediate depth (a_{12} = 19.6 mm). The latter depth was determined from measured displacements and analysis and was confirmed by the appearance of the fracture surface. The crack was at its intermediate depth from point B to C; during the time from C to D, it grew by tearing from a depth of 19.6 to 22.5 mm. The crack propagated by cleavage (D to E) and subsequently tore to a depth of 42.4 mm. The K_{Ic}-vs-time curves shown in Fig. 17 were calculated from the measured temperatures for two crack depths on the basis of the upper-toughness K_{Ic} curve of Fig. 15 shifted by ~20°K to agree with the cleavage initiation event in PTSE-2B. Figure 17 shows that the crack attained the $K_I > K_{Ic}$ condition during the warm-prestressing phase, B to C, as had been planned.

In the second transient (PTSE-2B) the crack initially tore to a depth of 46.1 mm before cleavage. The conditions of the cleavage fracture in PTSE-2B are shown in Fig. 18. The K_I curve is for the precleavage crack

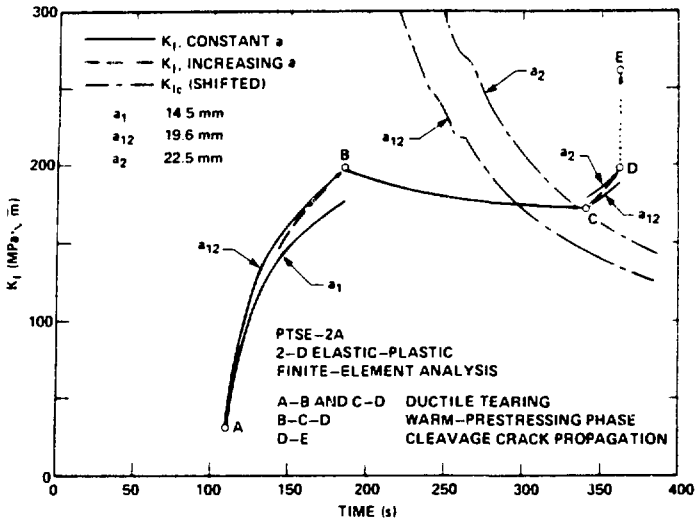

Fig. 17. K_I and K_{Ic} vs time from posttest elastic-plastic finite-element analyses based on actual pressure and temperatures measured in PTSE-2A for precleavage crack depths.

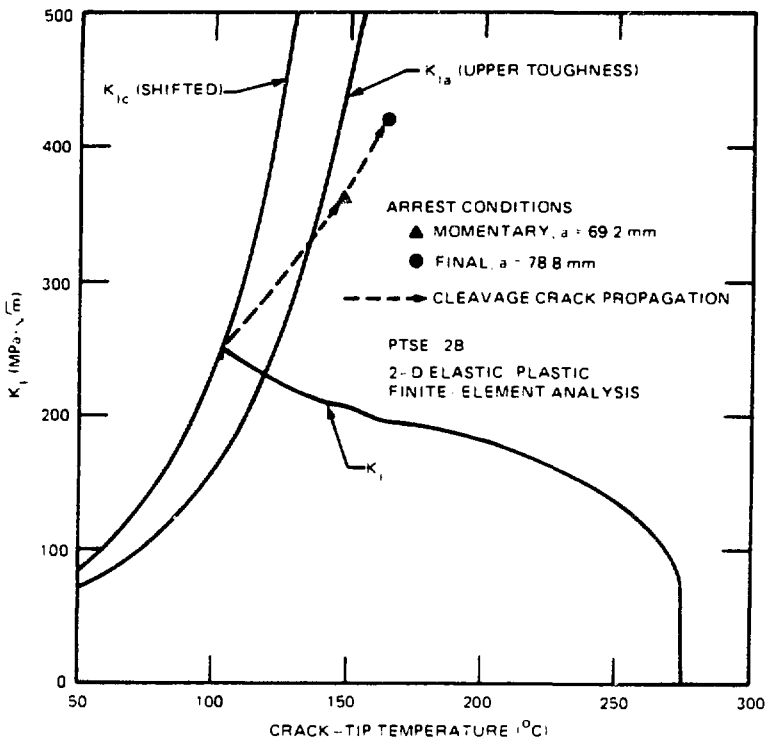

Fig. 18. Crack-tip conditions for precleavage crack depth from posttest elastic-plastic finite-element analysis using experimental pressure and temperature data from transient PTSE-2B: K_I, K_{Ic}, and K_{Ia} vs crack-tip temperature.

depth, 46.1 mm. The momentary arrest at 69.2 mm was evident only by the long narrow band of ductile tearing visible on the fracture surface (Fig. 16).

The toughness values K_{Ic} and K_{Ia} inferred from the experimental data are shown in Fig. 19 in comparison with the pretest upper-toughness K_{Ia} curve, and the upper K_{Ic} curve shifted to agree with PTSE-2B. The apparent elevation of the PTSE-2A initiation point as a consequence of warm prestressing is ~50 MPa•√m.

The crack initiation after warm prestressing in PTSE-2A was interpreted on the basis of a theoretical procedure developed by Chell [12]. For application to PTSE-2, Chell's theory was modified to account for tearing during the final loading step. The modification is similar to that described by Chell in Ref. 13. The analysis described here involves simplification of the physical states of the real structure: the strip-yield model of plastic zones is used; the temperature and flow stresses at the crack tip are attributed to the entire plastic zones; the loading states are expressed in terms of K_I values calculated by a deformation theory plasticity model; and tearing is assumed to take place in a short time interval immediately preceding cleavage.

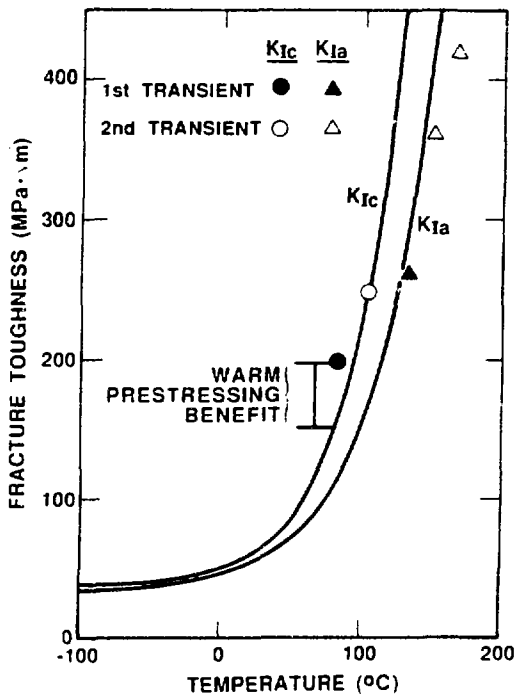

Fig. 19. Crack initiation (K_{Ic}) and arrest (K_{Ia}) toughness values observed in PTSE-2 compared with shifted pretest K_{Ic} curve and upper-toughness K_{Ia} curve.

The significant effects of warm prestressing with and without ductile tearing are illustrated in Fig. 20. The solid curves in Figs. 20(a) and (b) represent the theoretical predictions of K_I at fracture for a fixed crack and a tearing crack, respectively. The experimental point in Fig. 20(a) would be the perceived initiation condition if one did not know that the crack tore immediately prior to cleavage. For both the tearing and the fixed cracks, the theoretical and experimental fracture points exceed K_{Ic} substantially, namely, >40 MPa $\sqrt{m}$. The calculations for the tearing crack predicted that fracture would have occurred at a $K_I \simeq 7$ MPa$\cdot\sqrt{m}$ lower than the experimental point, as shown in Fig. 20(b). When tearing is involved, the predicted fracture conditions are very sensitive to the extent of tearing and the tensile strength of the material.

The low-tearing resistance of the PTSE-2 material promoted ductile tearing in both transients. The tearing occurred while material at the crack tip was at or below the onset of the Charpy upper shelf. The tearing behavior in PTSE-2 was remarkably different from that of PTSE-1, in which there was no contiguous region of ductile tearing. The extent of tearing was estimated for both experiments on the assumption that

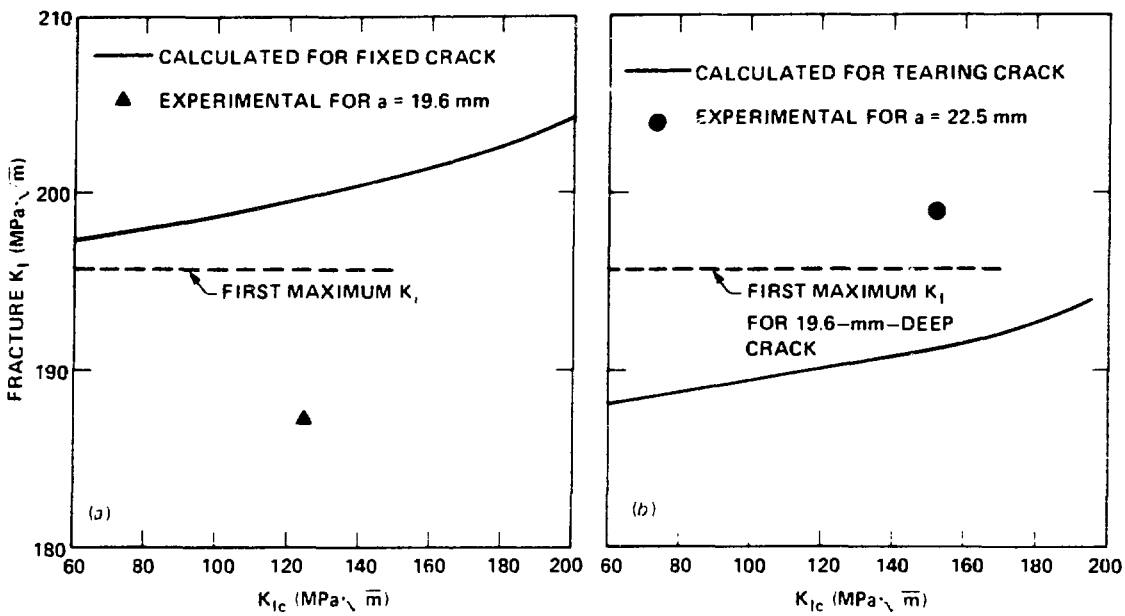

Fig. 20. Theoretical prediction of post-warm-prestressing fracture conditions K_I vs K_{Ic} for PTSE-2A transient compared with actual fracture. Predictions are based on K_I values from posttest elastic-plastic finite-element analysis using measured pressure and temperatures. Plastic zones in the warm-prestressing analysis are based on measured flow stresses for characterization material PTC1. (a) Crack without tearing, (b) tearing crack.

stable tearing is controlled by the condition $J_I = J_R$, where J_I and J_R are the applied J-integral and the tearing resistance, respectively. The applied J-integral was computed both from J based on deformation theory [14] and J modified by Ernst [15]. Although J_R was much higher for PTSE-1 than PTSE-2, measurable tearing was predicted from J_R data for that experiment. Within the scatter of J_R-Δa data presented in Fig. 13, calculated values of Δa that agree with the PTSE-2 experiment can be found. However, no single J_R-Δa curve can predict all of the stable crack extensions in PTSE-2.

5. SUMMARY AND CONCLUSIONS

Results from the PTSE test data indicate that the ASME *Boiler and Pressure Vessel Code* Sect. XI toughness relations are conservative relative to actual material characteristics. The experiments demonstrated that arrest toughness values substantially above the cutoff of Sect. XI (220 MPa $\cdot \sqrt{m}$) could be realized. In PTSE-1, the highest value of arrest occurred at a temperature about 30°K above the onset of the Charpy upper shelf. This is believed to be very close to the threshold temperature above which cleavage fracture cannot persist. This result also suggests that the methods of linear elastic fracture mechanics have an important role in fracture evaluation at high (upper-shelf) temperatures. The PTSE-2 test demonstrated that low-upper-shelf material can also exhibit very high arrest toughness values. This trend for increasing arrest toughness values with increasing temperature (and consistently above the ASME Sect. XI K_{IR} curve) is also the case for several other large-scale test [16-20] as shown in Fig. 21, which includes the PTSE results. The materials represented in Fig. 21 have RT_{NDT} values that differ by more than 120°C.

The PTSE-1A and -1B transients were a demonstration that simple warm prestressing ($\dot{K}_I < 0$) strongly inhibits crack initiation. With allowance for uncertainty in the true K_{Ic} values it was evident that K_I exceeded K_{Ic} during warm prestressing by 50—90%. In transient A, simple antiwarm prestressing ($\dot{K}_I > 0$) prevailed during two periods of 40 s and 60 s duration without crack initiation, although K_I exceeded K_{Ic} by 30—50%. Clearly simple antiwarm prestressing ($\dot{K}_I > 0$) is not a sufficient condition to alleviate the effects of warm prestressing. The PTSE-2 experiment produced, for the first time with stress and toughness states representative of reactor pressure vessel, a brittle fracture following warm prestressing. The PTSE-2A transient demonstrated that (1) warm prestressing inhibits brittle fracture to some degree even when crack-driving forces are increasing with time; (2) benefits of warm prestressing are diminished by ductile tearing; and (3) a simple theoretical analyses of warm prestressing represented fracture conditions reasonably well.

In PTSE-1, a narrow band of ductile tearing formed ahead of the initial cleavage fracture. This was not unexpected, since analysis as well as prior intermediate vessel tests [11—13] indicated the potential for stable tearing prior to cleavage. The complete absence of ductile tearing after crack arrest is not consistent with tearing analysis based on

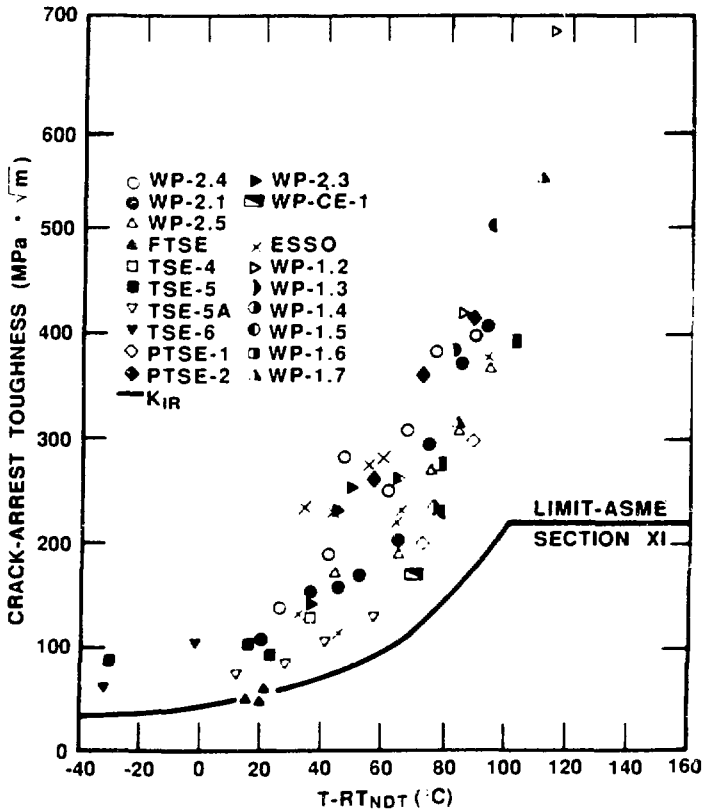

Fig. 21. High-temperature crack-arrest toughness data versus temperature ($T-RT_{NDT}$) for large specimen tests.

pretest data on tearing resistance. In the low-upper-shelf material of PTSE-2, ductile tearing preceded the onset of cleavage while the material at the crack-tip was at or below temperatures corresponding to the onset of the Charpy upper shelf. The ductile tearing had the effect of promoting more severe fractures in the material. Calculations of ductile tearing based on resistance curve test data for the PTSE-2 material performed with J based on deformation theory and J modified by Ernst did not consistently predict the tearing observed in the two transients.

REFERENCES

1. R. H. Bryan et al., *Pressurized-Thermal-Shock Test of 6-in.-Thick Pressure Vessels. PTSE-1: Investigations of Warm Prestressing and Upper-Shelf Arrest*, NUREG/CR-4106 (ORNL-6135), Martin Marietta Energy Systems, Inc., Oak Ridge Natl. Lab., April 1985.

2. "Rules for In-Service Inspection of Nuclear Power Plant Components," *ASME Boiler and Pressure Vessel Code, Section XI*, American Society of Mechanical Engineers, New York, 1983.

3. R. H. Bryan et al., *Pressurized-Thermal-Shock Test of 6-in.-Thick Pressure Vessels. PTSE-2: Investigation of Low Tearing Resistance and Warm Prestressing*, NUREG/CR-4888 (ORNL-6377), Martin Marietta Energy Systems, Inc., Oak Ridge Natl. Lab., December 1987.

4. R. Johnson, *Resolution of the Task A-11 Reactor Vessel Materials Toughness Safety Issue*, NUREG-0744, Vols, 1 and 2, Rev. 1, U.S. Nuclear Regulatory Commission, Washington, D.C., October 1982.

5. B. R. Bass and J. W. Bryson, *Applications of Energy Release Rate Techniques to Part-Through Cracks in Plates and Cylinders, Vol. 1. ORMGEN-3D: A Finite-Element Mesh Generator for 3-Dimensional Crack Geometries*, NUREG/CR-2997, Vol. 1 (ORNL/TM-8527/V1), Oak Ridge National Laboratory, Oak Ridge, TN (December 1982).

6. K. J. Bathe, *ADINA — A Finite Element Program for Automatic Dynamic incremental Nonlinear Analysis*. Report 82448-1, Massachusetts Institute of Technology, Cambridge, MA, September 1975 (revised December 1978).

7. B. R. Bass and J. W. Bryson, *Applications of Energy Release Rate Techniques to Part-Through Cracks in Plates and Cylinders, Vol. 2. ORVIRT: A Finite Element Program for Energy Release Rate Calculations for 2-D and 3-D Crack Models*, NUREG CR-2997, Vol. 2 (ORNL/TM-8527/V2). Oak Ridge National Laboratory, Oak Ridge, TN (February 1983).

8. R. H. Bryan and J. G. Merkle, Upper-shelf arrest analysis based on J_R-controlled tearing, in *Heavy-Section Steel Technology Program Quart. Prog. Rep. January–March 1983*, NUREG/CR-3334, Vol. 1 (ORNL/TM-8787/V1), pp. 111–124. Oak Ridge National Laboratory, Oak Ridge, TN (September 1983).

9. J. G. Merkle, *An Examination of the Size Effects and Data Scatter Observed in Small-Specimen Cleavage Fracture Toughness Testing*, ORNL/TM-9088, Union Carbide Corp. Nuclear Div., Oak Ridge Natl. Lab, April 1984.

10. F. J. Loss, "Toughness and Ductile Tearing Properties of Irradiated Low-Shelf Weld Metals," Nuclear Regulatory Commission 8th Water Reactor Safety Research Information Meeting, Gaithersburg, Maryland, October 27–31, 1980.

11. A. L. Hiser, F. J. Loss, and B. H. Menke, *J-R Curve Characterization of Irradiated Low Upper Shelf Welds*, NUREG/CR-3506 (MEA-2028), Materials Engineering Associates, Inc., Lanham, Maryland, April 1984.

12. G. G. Chell, "Some Fracture Mechanics Applications of Warm Prestressing to Pressure Vessels," Paper C22/80, pp. 117–24 in *Proc. 4th Int. Conf. on Pressure Vessel Technology*, I. Mech. E., London, 1980.

13. G. G. Chell, "The Effects of Sub-Critical Crack Growth on the Fracture Behavior of Cracked Ferritic Steels After Warm Prestressing," *Fatigue Fract. Engng. Mater. Struct.* 9(4), 259–74 (1986).

14. ASTM Standard E813-81, "Standard Test Method for J_{Ic}, A Measure of Fracture Toughness," pp. 762–80 in *1983 Annual Book of ASTM Standards*, American Society for Testing and Materials, Philadelphia, 1983.

15. H. A. Ernst, "Material Resistance and Instability Beyond J-Controlled Crack Growth," pp. 191–213 in *Elastic-Plastic Fracture: Second Symposium*, ASTM STP 803, Vol. I, American Society for Testing and Materials, Philadelphia, 1983.

16. D. J. Naus et al., *Crack Arrest Behavior in SEN Wide Plates of Quenched and Tempered A533B Steel Tested under Nonisothermal Conditions*, NUREG/CR-4930 (ORNL-6388), Martin Marietta Energy Systems, Inc., Oak Ridge Natl. Lab., September 1987.

17. D. J. Naus et al., "Summary of HSST Wide-Plate Crack-Arrest Tests and Analyses," *Proc. of U.S. Nuclear Regulatory Commission Fifteenth Water Reactor Safety Information Meeting held at National Bureau of Standards*, Gaithersburg, Maryland, NUREG/CP-0091, pp. 17–40, February 1988.

18. R. D. Cheverton et al., "Fracture Mechanics Data Deduced from Thermal-Shock and Related Experiments with LWR Pressure Vessel Material," *J. Pressure Vessel Technol.* 105, 102-10 (May 1983).

19. Japan Welding Council, *Structural Integrity of Very Thick Steel Plate for Nuclear Reactor Pressure Vessels*, JWES-AE-7806, Tokyo, 1977 (in Japanese).

20. A. Pellissier-Tanon, P. Sollogoub, and B. Houssin, "Crack Initiation and Arrest in an SA 508 Class-3 Cylinder Under Liquid Nitrogen Thermal-Shock Experiment," *Transactions of the 7th International Conference on Structural Mechanics in Reactor Technology*, Chicago, Vols. G and H, 132–42 (August 1983).

21. R. W. Derby et al., *Test of 6-in.-Thick Pressure Vessels. Series 1: Intermediate Test Vessels V-1 and V-2*, ORNL-4895. Oak Ridge National Laboratory, Oak Ridge, TN (February 1974).

22. R. H. Bryan et al., *Test of 6-in.-Thick Pressure Vessels, Series 2: Intermediate Test Vessels V-3, V-4, and V-6*, ORNL-5059, Oak Ridge National Laboratory, Oak Ridge, TN (November 1975).

23. J. G. Merkle et al., *Test of 6-in.-Thick Pressure Vessels. Series 4: Intermediate Test Vessels V-5 and V-9*, ORNL/NUREG-7. Oak Ridge National Laboratory, Oak Ridge, TN (August 1977).